

# UC Santa Barbara

## UC Santa Barbara Previously Published Works

### Title

Desymmetrization and Parallel Kinetic Resolution of 1-Ethynylcyclobutanols via Asymmetric Cooperative Gold Catalysis

### Permalink

<https://escholarship.org/uc/item/7w51s9r3>

### Journal

Journal of the American Chemical Society, 145(50)

### ISSN

0002-7863

### Authors

Zhao, Ke

Yang, Ziguang

Yang, Jieli

et al.

### Publication Date

2023-12-20

### DOI

10.1021/jacs.3c09288

Peer reviewed



Published in final edited form as:

*J Am Chem Soc.* 2023 December 20; 145(50): 27205–27210. doi:10.1021/jacs.3c09288.

## Desymmetrization and Parallel Kinetic Resolution of 1-Ethynylcyclobutanols via Asymmetric Cooperative Gold Catalysis

**Ke Zhao<sup>‡</sup>,**

Department of Chemistry and Biochemistry, University of California, Santa Barbara, California 93117, United States

**Ziguang Yang<sup>‡</sup>,**

Department of Chemistry and Biochemistry, University of California, Santa Barbara, California 93117, United States

**Jielin Yang,**

Department of Chemistry and Biochemistry, University of California, Santa Barbara, California 93117, United States

**Xinyi Li,**

Department of Chemistry and Biochemistry, University of California, Santa Barbara, California 93117, United States

**Carlos D. Quintanilla,**

Department of Chemistry and Biochemistry, University of California, Santa Barbara, California 93117, United States

**Liming Zhang**

Department of Chemistry and Biochemistry, University of California, Santa Barbara, California 93117, United States

### Abstract

Enantioselective gold catalysis remains a challenging area of research. By harnessing gold–ligand cooperation in the presence of a chiral bifunctional phosphine ligand featuring a novel 3'-phosphine oxide moiety, highly enantioselective desymmetrization of 1-ethynylcyclobutanols

**Corresponding Author: Liming Zhang** – Department of Chemistry and Biochemistry, University of California, Santa Barbara, California 93117, United States; zhang@chem.ucsb.edu.

<sup>‡</sup>K.Z. and Z.Y. made equal contribution to this work.

#### Supporting Information

The Supporting Information is available free of charge at <https://pubs.acs.org/doi/10.1021/jacs.3c09288>.

Detailed experimental procedures, mechanistic studies, X-ray structure, DFT optimized structures, chiral HPLC chromatographs, and NMR spectra. (PDF)

#### Accession Codes

CCDC 2280655–2280656 contain the supplementary crystallographic data for this paper. These data can be obtained free of charge via [www.ccdc.cam.ac.uk/data\\_request/cif](http://www.ccdc.cam.ac.uk/data_request/cif), or by emailing [data\\_request@ccdc.cam.ac.uk](mailto:data_request@ccdc.cam.ac.uk), or by contacting The Cambridge Crystallographic Data Centre, 12 Union Road, Cambridge CB2 1EZ, UK; fax: +44 1223 336033.

Complete contact information is available at: <https://pubs.acs.org/doi/10.1021/jacs.3c09288>

The authors declare no competing financial interest.

is achieved, permitting access to chiral  $\alpha$ -methylene cyclopentanones featuring a diverse array of chiral quaternary and tertiary centers. This cooperative gold catalysis also enables parallel kinetic resolution in gold catalysis, delivering cyclopentanone regioisomers with excellent enantiomeric excesses. DFT calculations of the transition states support the distinct mechanism of asymmetric induction via controlling the conformation of the bound substrate and hence dictating the ring bond undergoing migration.

Despite much success in achieving enantioselective gold chemistry in the past,<sup>1–10</sup> the linear configuration of ligand–Au<sup>I</sup>–substrate and hence the difficulty in imposing a ligand chiral environment at the reaction site still pose a challenge to further advances in this important aspect of gold catalysis.<sup>11–13</sup> For the past several years we have developed several bifunctional biaryl-2-ylphosphine ligands for gold–ligand cooperative catalysis (Scheme 1A).<sup>14</sup> The participation of the ligand remote basic functional group in bond-forming/breaking events in this class of versatile catalysis<sup>15–18</sup> offers unique opportunities to achieve asymmetric gold catalysis. This strategy is facilitated by the ease of access to the chiral binaphthyl framework from commercial chiral binols.<sup>19</sup> For example, the chiral version of WangPhos featuring a remote amide group, i.e. (*R*)-**L1**, was initially prepared in 4 steps from (*R*)-binol<sup>20</sup> and later in 5 steps in a more reliable and divergent approach.<sup>19</sup> By using (*R*)-**L1** as the ligand, the cyclization of allenols is asymmetrically accelerated due to the metal–ligand cooperation phenomenon and exhibits high levels of enantioselectivity while with a catalyst loading of as low as 100 ppm (Scheme 2B).<sup>20</sup> A facile asymmetric dearomatization was later realized by using either an amide or a phosphonate as the remote basic group.<sup>19,21</sup> Both of these studies utilize a key H-bonding interaction between the basic group and substrates to facilitate and organize the enantioselective nucleophilic cyclization. In this work, we disclose a distinctively different approach to harnessing asymmetric gold–ligand cooperation: that is, asymmetric ring enlargement via H-bond-dictated substrate conformation control. The concept is shown in Scheme 1C, where 1-ethynylcyclobutanols could undergo ring expansion to form  $\alpha$ -methylene cyclopentanone products.<sup>22</sup> The racemic/achiral version of this chemistry was reported by Toste in 2005.<sup>23</sup> In this asymmetric transformation, as outlined in structure **A**, the H-bond between the ligand basic group and the substrate HO group would control the rotation of the C(sp)–C(sp<sup>3</sup>) bond in red to orient the migrating ring C(sp<sup>3</sup>)–C(sp<sup>3</sup>) bond in blue to be antiperiplanar to the gold–alkyne interaction. As such, its selective migration would be achieved, leading to desymmetrization or kinetic resolution. In addition, the H-bonding interaction should also accelerate the ring expansion by accommodating the proton generated in the process. Due to the distal nature of the prochiral center at cyclobutanol ring C3, the desymmetrization approach would permit ready access to various quaternary and tertiary chiral centers.

We began the study by examining the desymmetric ring expansion of the 1-ethynylcyclobutanol **1a** possessing a quaternary carbon center at the ring C3 position. Its HO group is *cis* to the TBS-protected hydroxymethyl group. This relative stereochemistry is confirmed by single-crystal X-ray diffraction studies of the corresponding diol.<sup>24</sup> By using the binaphthyl-2-ylphosphine ligand (*S*)-**L2** featuring a distal *N,N*-dimethylamide group, the desired ring expansion did occur, affording the cyclopentanone product **2a** in 89% ee (Table 1, entry 1). However, the reaction yield was only 33%. The intermolecular reaction between

the C–C triple bond and the tertiary alcohol moiety was posited as the major side reaction. By sequentially diluting the reaction, the yield was improved to 46% and 58%, respectively (entries 2 and 3). We then screened (*S*)-**L1**, (*S*)-**L3**, and (*S*)-**L4**, and the diphenylphosphine oxide functionalized ligand (*S*)-**L5** (entries 4–7). The last ligand is a new addition to this class of remotely functionalized bifunctional ligands and performed noticeably better than the amide ligands [i.e., (*S*)-**L1**–**L3**] and the phosphonate ligand (*S*)-**L4**. Subsequent tuning of the electronics of the phenyl groups of **L5** revealed that **L6** with electron-donating MeO groups performed worse (entry 8) and that **L7** with moderately electron-withdrawing chloro groups resulted in the same ee value but a substantially improved yield (90%, entry 9). When running in toluene, the reaction was lowyielding, although the enantioselectivity (91%) remained excellent (entry 10). Changing  $\text{BAR}^{\text{F}}_4^-$  to  $\text{NTf}_2^-$  led to erosion of the yield and enantioselectivity (entry 11). We also tried the reaction using the unfunctionalized ligand (*S*)-**L0**. Although most of the substrate was consumed, only a trace product was detected. This result confirms the additional role of the remote basic group in accelerating/promoting the ring expansion. In a preparative scale reaction, **2a** was isolated in 95% yield with 90% ee (entry 13). As expected, under the same conditions, the reaction of *trans*-**1a** afforded the opposite product enantiomer in a comparable yield and enantioselectivity (entry 14).

With the optimal conditions (Table 1, entry 9) in hand, we proceeded to explore the reaction scope. We first examined achiral 1-ethynylcyclobutanols **1** bearing a quaternary carbon center at the ring 3 position. As shown in Table 2, a variety of functional groups were tolerated in the cases of **2b–2j**. They include esters of different types (**2b**, **2g**, and **2h**), C–C double bonds including allyl (**2d**), vinyl (**2f**), and electron-deficient C–C double bond (**2h**), ketone carbonyl (**2j**), and NBoc (**2i**). The reaction yields range from 75% to 96%, and the enantiomeric excesses are mostly around or above 90%. In the case of **2e** possessing a sterically hindered isopropyl-substituted quaternary center, the ee was 85%. In some cases, a slightly elevated reaction temperature (i.e., 40 °C) was employed to accelerate the reaction. Similar to the case of **2a**, by using the substrate *cis* and *trans* diastereomers, both enantiomers of the acetate **2b** were isolated in 90% ee, respectively. We then employed substrates containing a monosubstituted C3 center. The reactions led to 2-methylenecyclopentanones **2k–2o** possessing a chiral tertiary center at C4 in good to excellent yields and with mostly excellent enantioselectivities. Different C4 substituents, including silyl-protected hydroxy groups (**2k** and **2o**), phenyl (**2l**), and bulky *tert*-butyl (**2m**) were readily tolerated. Interestingly, the unprotected tertiary alcohol in **2n** was allowed, and the reaction was slightly slower, which can be attributed to the competing H-bonding interaction between the tertiary alcohol and the phosphine oxide in the ligand. What is remarkable about this chemistry is that it permits the creation of all-carbon quaternary chiral centers of a range of synthetically valuable substitution patterns, including being at allylic (**2f** and **2h**), homoallylic (**2d**), alpha to ester (**2g**) and ketone (**2j**), and beta to heteroatoms (**2a–2c** and **2i**).

We were curious whether our catalytic system could achieve kinetic resolution of racemic 1-ethynylcyclobutanol with a substitution at the ring C2 position. As shown in Scheme 2, when the racemic *trans*-**1p** with the hydroxyl group *trans* to the ring C2 substituent

was treated by catalytic  $\mathbf{L2Au}^+$ , we observed the formation of two cyclopentenone regioisomers, i.e.,  $\mathbf{2p}$  and  $\mathbf{2p}'$  in equal amounts and a combined 95% yield. Moreover, both exhibited 96% enantiomeric excess. These surprising results reveal that our catalytic system achieves parallel kinetic resolution,<sup>25–27</sup> in which the (1*R*,2*S*)- $\mathbf{1p}$  is stereoselectively isomerized to (*S*)- $\mathbf{2p}$  and (1*S*,2*R*)- $\mathbf{1p}$  to the regioisomer (*R*)- $\mathbf{2p}'$ . It is noteworthy that the *N,N*-dimethylamide ligand  $\mathbf{L2}$  is the optimal ligand and no gold-catalyzed parallel kinetic resolution is rare; moreover, the preferred migration of more substituted groups<sup>23</sup> is overruled by the catalyst. Electronic perturbation of the phenyl group of  $\mathbf{1p}$  by a  $\text{CF}_3$  or MeO group was then probed. Racemization of (*S*)- $\mathbf{2q}$  possessing an electron-withdrawing  $\text{CF}_3$  group was observed under the standard conditions including the use of excess  $\text{NaBAR}_4^{\text{F}_4}$  ( $2 \times \text{Au}$  loading). This is likely due to the Lewis acidity of  $\text{Na}^+$  and the increased acidity of the ketone  $\alpha$ -hydrogen of (*S*)- $\mathbf{2q}$ . By using  $\text{AgNTf}_2$  (stoichiometric to Au) as the chloride scavenger, 92% ee was achieved for both (*S*)- $\mathbf{2q}$  and its regioisomer (*R*)- $\mathbf{2q}'$ . In comparison, the MeO case resulted in the formation of (*S*)- $\mathbf{2r}$  and (*R*)- $\mathbf{2r}'$  with higher ee values and excellent yields while using  $\text{NaBAR}_4^{\text{F}_4}$  as the chloride scavenger. Functional groups such as vinyl [(*R*)- $\mathbf{2s}$ /(*S*)- $\mathbf{2s}'$ ] and TIPS ether [(*S*)- $\mathbf{2t}$ /(*R*)- $\mathbf{2t}'$ ] were readily tolerated. The structure of the substrate *trans*- $\mathbf{1t}$  is confirmed by the X-ray single crystal structure of its diol counterpart.<sup>28</sup> In addition, a neopentyl group [(*S*)- $\mathbf{2u}$ /(*R*)- $\mathbf{2u}'$ ] had little impact on the regioselectivity (~1:1) and the enantioselectivities. On the other hand, the case with a sterically demanding isopropyl group [(*S*)- $\mathbf{2v}$  and (*R*)- $\mathbf{2v}'$ ] required running the reaction at 0 °C for 18 h to achieve good to excellent resolution. The *R*-configuration of  $\mathbf{2v}'$  was established by comparing its optical rotation with the literature report,<sup>29,30</sup> and the absolute configurations of the other products in this series are assigned accordingly.

We conducted mechanistic studies of the reaction of *trans*- $\mathbf{1t}$  to understand this parallel kinetic resolution phenomenon. First, a control experiment using *trans*- $\mathbf{1t}$  and the unfunctionalized ligand (*S*)- $\mathbf{L0}$  afforded  $\mathbf{2t}$  and  $\mathbf{2t}'$  in low yields and a ratio of 1:1.25 after 60 h (Scheme 3A). Moreover, these products exhibited low enantiomeric excesses in the opposite sense. We then monitored the parallel kinetic resolution reaction over time using (*S*)- $\mathbf{L2}$  as the ligand (Scheme 3B). The initial formation of (*S*)- $\mathbf{2t}$  was noticeably faster than (*R*)- $\mathbf{2t}'$ , but not sufficient to realize typical kinetic resolution. Interestingly, when we monitored the reaction progress of racemic *cis*- $\mathbf{1t}$ , a large rate difference in the formation of the two regioisomeric products was observed. As such, a typical kinetic resolution was achieved when *cis*- $\mathbf{1t}$  was subjected to the standard conditions; with the reaction halted at 61% conversion, (*S*)- $\mathbf{2t}'$  was afforded in 42% yield and in 83% ee, while 39% of the unreacted (1*R*, 2*R*)- $\mathbf{1t}$  remained, and its ee is 85%.

The two transition states leading to the opposite enantiomers of cyclopentanone product  $\mathbf{2f}$  in this desymmetrization reaction were located by DFT calculations and are shown in Figure 1A.  $\text{NTf}_2^-$  instead of  $\text{BAR}_4^{\text{F}_4-}$  was employed as the counteranion in order to simplify the calculation and permit hydrogen bonding with the substrate in both scenarios. As evident in Table 1, entries 9 and 11, the switching of the counteranions has only a minor impact on enantioselectivity. In the favored transition state (i.e., **B**) leading to the formation of the major enantiomer of  $\mathbf{2f}$ , the ligand phosphine oxide forms a strong H-bonding interaction [ $d(\text{O}' \cdots \text{H}) = 1.5667 \text{ \AA}$ ] with the substrate hydroxyl group, and the H–O bond ( $d = 1.0040$

Å) in the substrate experiences notable elongation. As predicted, this H-bonding interaction facilitates selective migration of one of the cyclobutane ring C–C bonds by positioning it antiperiplanar to the gold–alkyne interaction via conformational control. Of note, the counteranion  $\text{NTf}_2^-$  does not engage in H-bond interaction with the substrate HO group. On the other hand, in the transition state C disfavored by 10.1 kcal/mol and leading to the minor enantiomer, the substrate HO group forms a H-bonding interaction with  $\text{NTf}_2^-$ , but the N...H distance - 1.6249 Å - is notably longer than that of O'...H in **B**, while the substrate OH bond ( $d = 1.0048$  Å) experiences a slight larger elongation. Although the energy difference of these two TSs is overestimated, the data are consistent with the fact that the ligand phosphine oxide plays a critical role in dictating the regioselective/desymmetric ring expansion and accelerating the overall reaction. Figure 1B depicts the four stereoisomers of 2-methylcyclobutanol (**1w**) and the DFT-calculated ring expansion barriers of the preferred reaction pathway using (*S*)-**L2** as the ligand. In the cases of the two enantiomers of *trans*-**1w**, the reaction barriers, 17.4 and 18.1 kcal/mol, are similar, consistent with the observed parallel kinetic resolution phenomenon. The absence of a much lower barrier in the preferred migration of a secondary alkyl group in the case of *trans*-**1w-2** in comparison to *trans*-**1w-1** is attributed to some steric clash between the methyl group and the reacting C–C triple bond in the transition state. On the other hand, the reaction of *cis*-**1w-2** experiences a free energy barrier of 17.2 kcal/mol, which is 3.8 kcal/mol lower than that of its enantiomer *cis*-**1w-1**. This phenomenon is consistent with the fact that the migration of a secondary alkyl group in *cis*-**1w-2** is more facile than that of a primary alkyl group in *cis*-**1w-1**, and the methyl group in *cis*-**1w-2** does not cause similar steric clash as it points away from the C–C triple bond.

In summary, an enantioselective desymmetrization of 1-ethynylcyclobutanols is achieved via asymmetric cooperative gold catalysis. The chemistry is enabled by a chiral bifunctional binaphthylphosphine ligand featuring a novel 3'-diarylphosphine oxide substituent.  $\alpha$ -Methylenecyclopentanones possessing a diverse range of quaternary and tertiary chiral centers are formed with excellent enantioselectivities. Moreover, this gold–ligand cooperation permits parallel kinetic resolution in gold catalysis, converting racemic 1-ethynylcyclobutanols into two regioisomeric cyclopentanones with excellent enantiomeric excesses. This work represents a distinct approach to harnessing metal–ligand cooperation and opens new opportunities for achieving asymmetric gold catalysis.

## Supplementary Material

Refer to Web version on PubMed Central for supplementary material.

## ACKNOWLEDGMENTS

The authors thank NIGMS R35GM139640 and NSF CHE 1800525 for financial support and NSF MRI-1920299 for the acquisition of Bruker 500 and 400 MHz NMR instruments. We thank Dr. Guang Wu and Dr. Yongliang Zhang for their help with the X-ray structures. The DFT calculations were conducted at the Center for Scientific Computing at UCSB, which is supported by NSF CNS-1725797, DMR 2308708 and OAC-1925717.

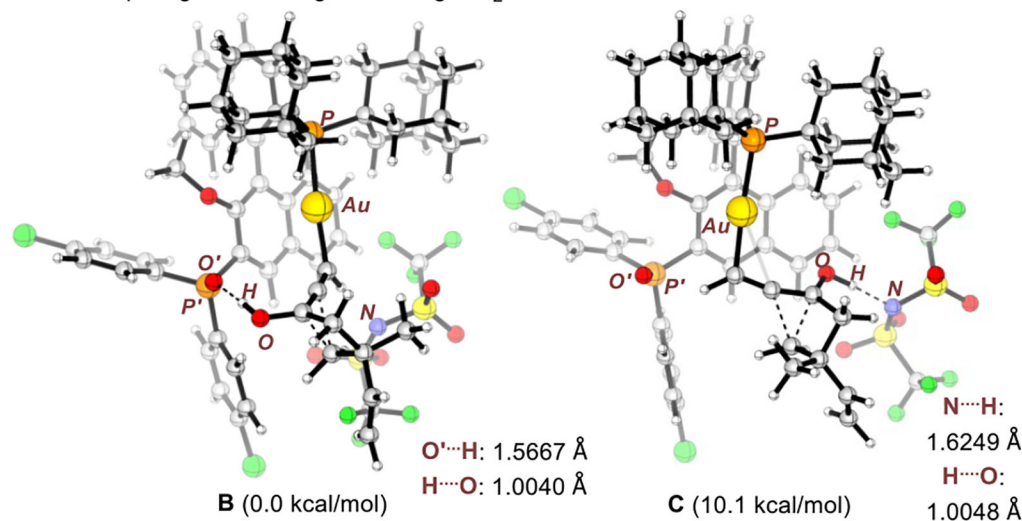
## REFERENCES

- (1). Zi W; Dean Toste F Recent Advances in Enantioselective Gold Catalysis. *Chem. Soc. Rev* 2016, 45, 4567–4589. [PubMed: 26890605]
- (2). Pradal A; Toullec PY; Michelet V Recent Developments in Asymmetric Catalysis in the Presence of Chiral Gold Complexes. *Synthesis* 2011, 2011, 1501–1514.
- (3). Sengupta S; Shi X Recent Advances in Asymmetric Gold Catalysis. *ChemCatChem*. 2010, 2, 609–619.
- (4). Das A; Patil NT Enantioselective C-H Functionalization Reactions under Gold Catalysis. *Chem.—Eur. J* 2022, 28, No. e202104371.
- (5). Li YY; Li WB; Zhang JL Gold-Catalyzed Enantioselective Annulations. *Chem.—Eur. J* 2017, 23, 467–512. [PubMed: 27723131]
- (6). Marinetti A; Jullien H. l. n. Voituriez A Enantioselective, Transition Metal Catalyzed Cycloisomerizations. *Chem. Soc. Rev* 2012, 41, 4884–4908. [PubMed: 22674143]
- (7). Toullec PY; Pradal A; Michelet V Recent Developments in Asymmetric Catalysis In Gold Catalysis: An Homogeneous Approach; Toste FD, Michelet V, Eds.; Imperial College Press: Singapore, 2014; pp 445–500.
- (8). Wang Y-M; Lackner AD; Toste FD Development of Catalysts and Ligands for Enantioselective Gold Catalysis. *Acc. Chem. Res* 2014, 47, 889–901. [PubMed: 24228794]
- (9). Gutman K; Zhang L Gold-Catalyzed Enantioselective Reactions. In Reference Module in Chemistry, Molecular Sciences and Chemical Engineering; Elsevier: 2023; 10.1016/B978-0-32-390644-9.00095-0.
- (10). Escofet I; Zuccarello G; Echavarren AM Gold-Catalyzed Enantioselective Cyclizations and Cycloadditions In *Advances in Organometallic Chemistry*; Academic Press: 2022.
- (11). Abu Sohail SM; Liu R-S Carbocyclisation of Alkynes with External Nucleophiles Catalysed by Gold, Platinum and Other Electrophilic Metals. *Chem. Soc. Rev* 2009, 38, 2269–2281. [PubMed: 19623349]
- (12). Hashmi ASK Gold-Catalyzed Organic Reactions. *Chem. Rev* 2007, 107, 3180–3211. [PubMed: 17580975]
- (13).rstner A; Davies PW Catalytic Carbophilic Activation: Catalysis by Platinum and Gold II Acids. *Angew. Chem., Int. Ed* 2007, 46, 3410–3449.
- (14). Cheng X; Zhang L Designed Bifunctional Ligands in Cooperative Homogeneous Gold Catalysis. *CCS Chem*. 2021, 3, 1989–2002.
- (15). Grützmacher H Cooperating Ligands in Catalysis. *Angew. Chem., Int. Ed* 2008, 47, 1814–1818.
- (16). Askevold B; Roesky HW; Schneider S Learning from the Neighbors: Improving Homogeneous Catalysts with Functional Ligands Motivated by Heterogeneous and Biocatalysis. *ChemCatChem*. 2012, 4, 307–320.
- (17). Khusnutdinova JR; Milstein D Metal–Ligand Cooperation. *Angew. Chem., Int. Ed* 2015, 54, 12236–12273.
- (18). Trincado M; tzmacher H Cooperating Ligands in Catalysis In *Cooperative Catalysis*; Wiley-VCH Verlag GmbH & Co. KGaA: 2015; pp 67–110.
- (19). Zhao K; Kohnke P; Yang Z; Cheng X; You S-L; Zhang L Enantioselective Dearomative Cyclization Enabled by Asymmetric Cooperative Gold Catalysis. *Angew. Chem., Int. Ed* 2022, 61, No. e202207518.
- (20). Wang Z; Nicolini C; Hervieu C; Wong Y-F; Zononi G; Zhang L Remote Cooperative Group Strategy Enables Ligands for Accelerative Asymmetric Gold Catalysis. *J. Am. Chem. Soc* 2017, 139, 16064–16067. [PubMed: 29058889]
- (21). Zhang Y; Zhao K; Li X; Quintanilla CD; Zhang L Asymmetric Dearomatization of Phenols Via Ligand-Enabled Cooperative Gold Catalysis. *Angew. Chem., Int. Ed* 2023, 62, No. e202309256.
- (22). Iwasawa N; Matsuo T; Iwamoto M; Ikeno T Rearrangement of 1-(1-Alkynyl)Cyclopropanols to 2-Cyclopentenones Via Their Hexacarbonyldicobalt Complexes. A New Use of Alkyne–Co<sub>2</sub>(Co)<sub>6</sub> Complexes in Organic Synthesis. *J. Am. Chem. Soc* 1998, 120, 3903–3914.

- (23). Markham JP; Staben ST; Toste FD Gold(I)-Catalyzed Ring Expansion of Cyclopropanols and Cyclobutanols. *J. Am. Chem. Soc* 2005, 127, 9708–9709. [PubMed: 15998074]
- (24). CCDC number: 2280656
- (25). Vedejs E; Chen X Parallel Kinetic Resolution. *J. Am. Chem. Soc* 1997, 119, 2584–2585.
- (26). Eames J Parallel Kinetic Resolutions. *Angew. Chem., Int. Ed* 2000, 39, 885–888.
- (27). Dehli JR; Gotor V Parallel Kinetic Resolution of Racemic Mixtures: A New Strategy for the Preparation of Enantiopure Compounds? *Chem. Soc. Rev* 2002, 31, 365–370. [PubMed: 12491751]
- (28). CCDC number: 2280655.
- (29). Ghosh S; Erchinger JE; Maji R; List B Catalytic Asymmetric Spirocyclizing Diels-Alder Reactions of Enones: Stereo-selective Total and Formal Syntheses of Alpha-Chamigrene, Beta-Chamigrene, Laurencenone C, Colletoic Acid, and Omphalic Acid. *J. Am. Chem. Soc* 2022, 144, 6703–6708. [PubMed: 35389217]
- (30). Sawada T; Nakada M Enantioselective Total Synthesis of (+)-Colletoic Acid Via Catalytic Asymmetric Intramolecular Cyclopropanation of an Alpha-Diazo-Beta-Keto Diphenylphosphine Oxide *Org. Lett* 2013, 15, 1004–7. [PubMed: 23398353]



A. The competing TSs leading to **2f** using  $\text{NTf}_2^-$  as the counterion



B. Energetics of the kinetic resolution TSs using a methyl-substituted substrate

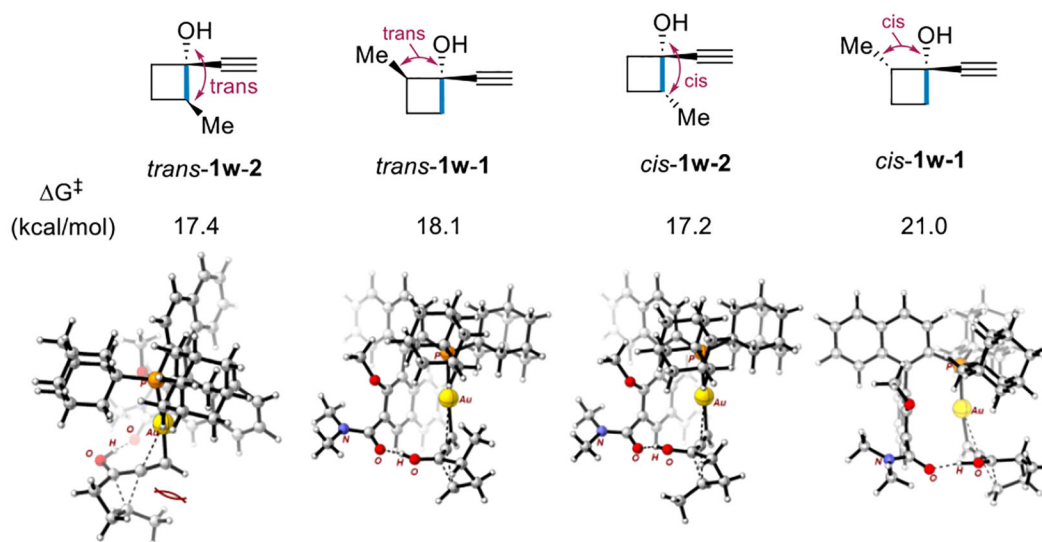
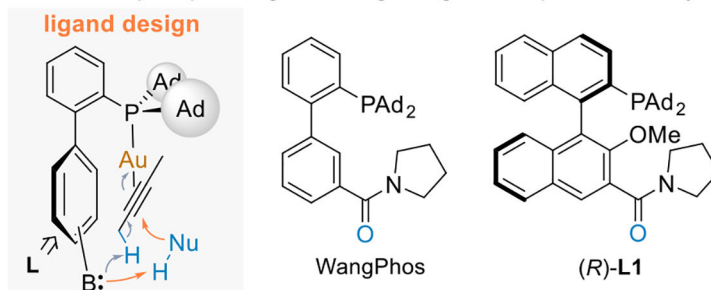


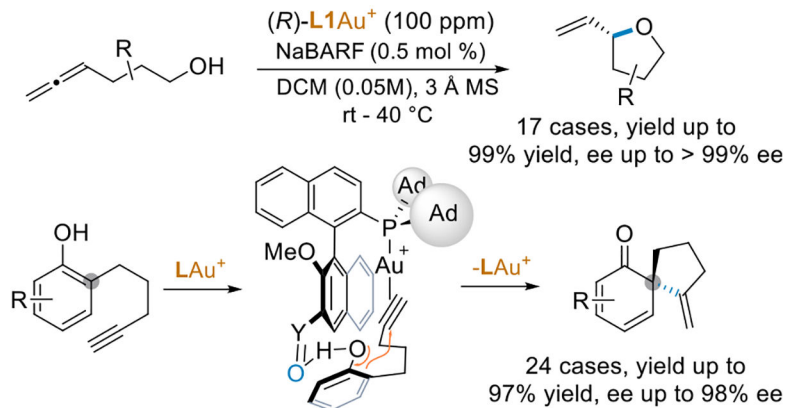
**Figure 1.**

DFT-calculated transition states at the M06/6-311G(d,p)/LAND2LZ(Au) level. Gibbs free energy shown.

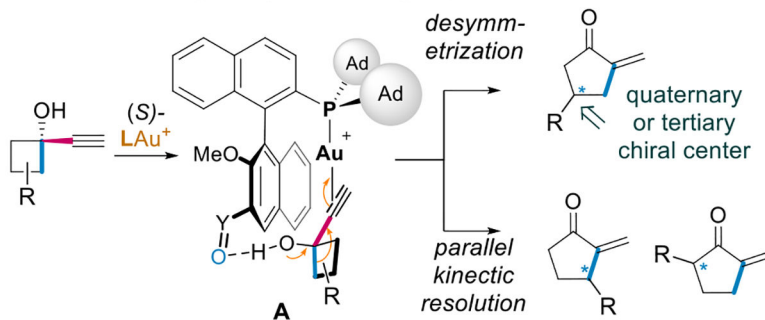
## A) Bifunctional phosphine ligands for gold-ligand cooperative catalysis



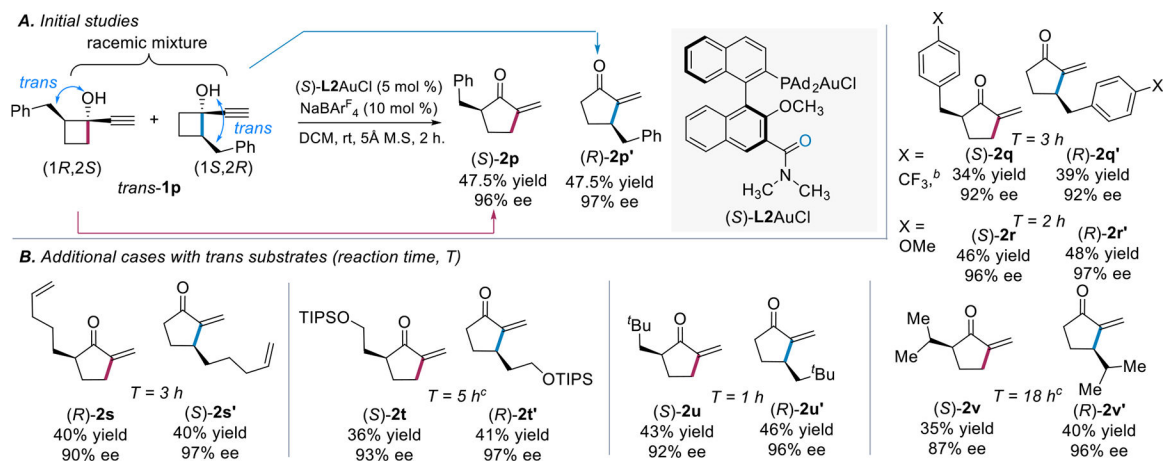
## B) Two examples of asymmetric cooperative gold catalysis



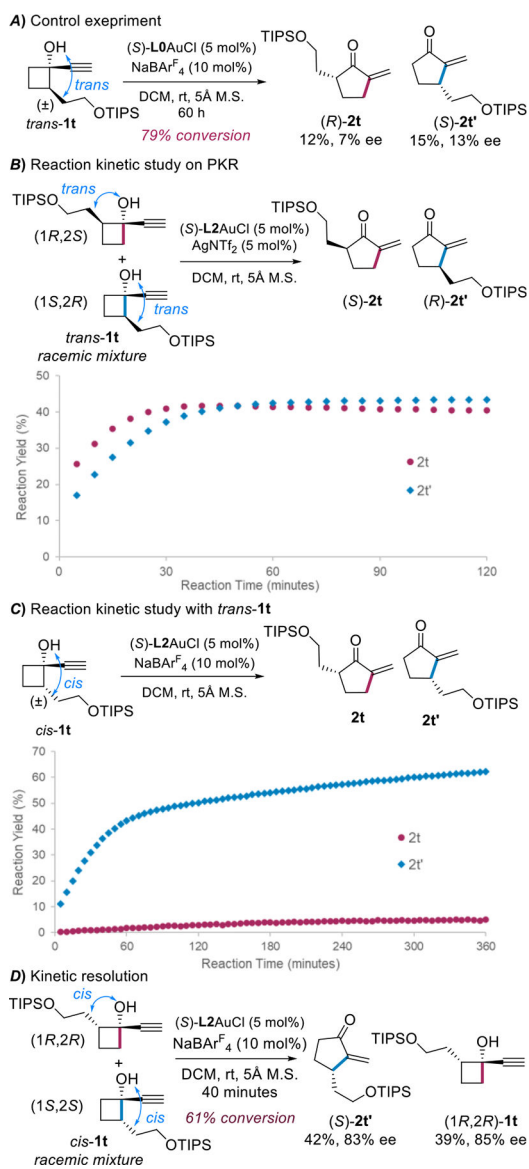
## C) This work: catalytic asymmetric ring expansion

**Scheme 1.**

Asymmetric Gold Catalysis Enabled by Metal-Ligand Cooperation

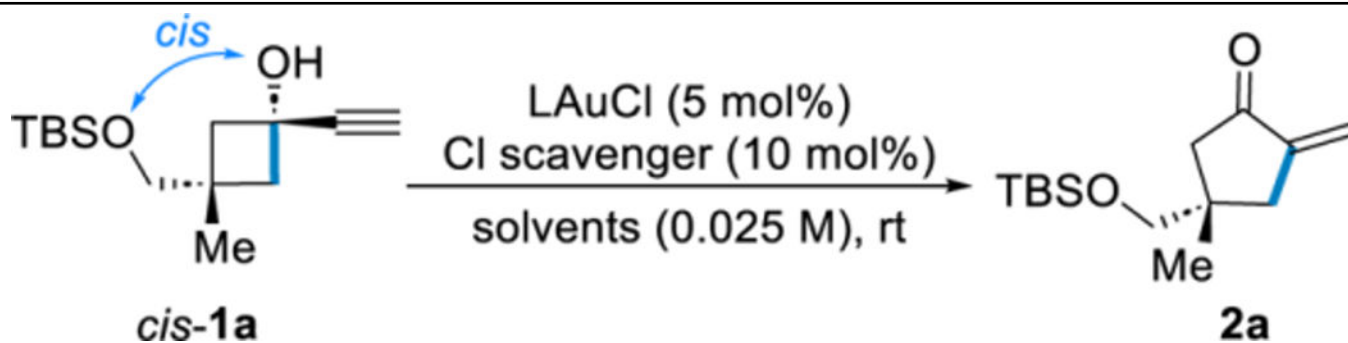
**Scheme 2.**Parallel Kinetic Resolution<sup>a</sup>

<sup>a</sup> Reaction run on a 0.20 mmol scale in DCM (0.025 M), the yield calculated based on the isolated mixture of regioisomers, and the ee values determined using TLC-purified materials. <sup>b</sup>5 mol % AgNTf<sub>2</sub> was used instead of NaBARF<sub>4</sub>. <sup>c</sup>Reaction was run at 0 °C.



**Scheme 3.**  
Mechanistic Studies

Table 1.

Optimization of the Reaction Conditions<sup>a</sup>

Entry	Catalyst	Solvent	yield <sup>b</sup>	ee <sup>c</sup>
1	( <i>S</i> )-L2AuCl/NaBAr <sup>F</sup> <sub>4</sub>	DCM (0.1 M)	33%	89%
2	( <i>S</i> )-L2AuCl/NaBAr <sup>F</sup> <sub>4</sub>	DCM (0.05 M)	46%	89%
3	( <i>S</i> )-L2AuCl/NaBAr <sup>F</sup> <sub>4</sub>	DCM	58%	90%
4	( <i>S</i> )-L1AuCl/NaBAr <sup>F</sup> <sub>4</sub>	DCM	63%	90%
5	( <i>S</i> )-L3AuCl/NaBAr <sup>F</sup> <sub>4</sub>	DCM	74%	89%
6	( <i>S</i> )-L4AuCl/NaBAr <sup>F</sup> <sub>4</sub>	DCM	64%	73%
7	( <i>S</i> )-L5AuCl/NaBAr <sup>F</sup> <sub>4</sub>	DCM	74%	91%
8	( <i>S</i> )-L6AuCl/NaBAr <sup>F</sup> <sub>4</sub>	DCM	69%	85%
9	( <i>S</i> )-L7AuCl/NaBAr <sup>F</sup> <sub>4</sub>	DCM	90%	91%
10	( <i>S</i> )-L7AuCl/NaBAr <sup>F</sup> <sub>4</sub>	toluene	36%	91%
11	( <i>S</i> )-L7AuCl/AgNTf <sub>2</sub>	DCM	61%	87%
12	( <i>S</i> )-L0AuCl/NaBAr <sup>F</sup> <sub>4</sub>	DCM	3% <sup>d</sup>	NA
13	( <i>S</i> )-L7AuCl/NaBAr <sup>F</sup> <sub>4</sub>	DCM	95% <sup>e</sup>	90%
14	( <i>S</i> )-L7AuCl/NaBAr <sup>F</sup> <sub>4</sub>	DCM	92% <sup>e,f</sup>	-90%

<sup>a</sup>Reaction condition: **1a** (0.05 mmol), LAuCl (5 mol %), NaBAr<sup>F</sup><sub>4</sub> (10 mol %), and 30 mg 5 Å MS in 2 mL of solvent, unless otherwise noted.

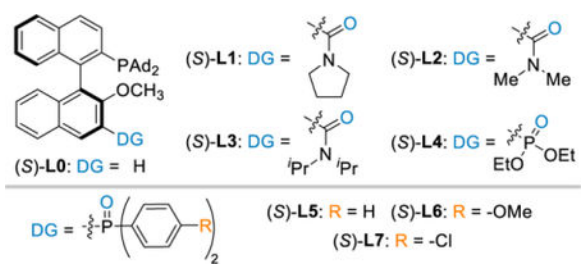
<sup>b</sup>Yields were determined by <sup>1</sup>H NMR analysis using diethyl phthalate as the internal standard.

<sup>c</sup>Determined by HPLC analysis.

<sup>d</sup>>97% reaction conversion.

<sup>e</sup>Isolated yield in 0.2 mmol scale.

<sup>f</sup>*Trans*-**1a** was used.



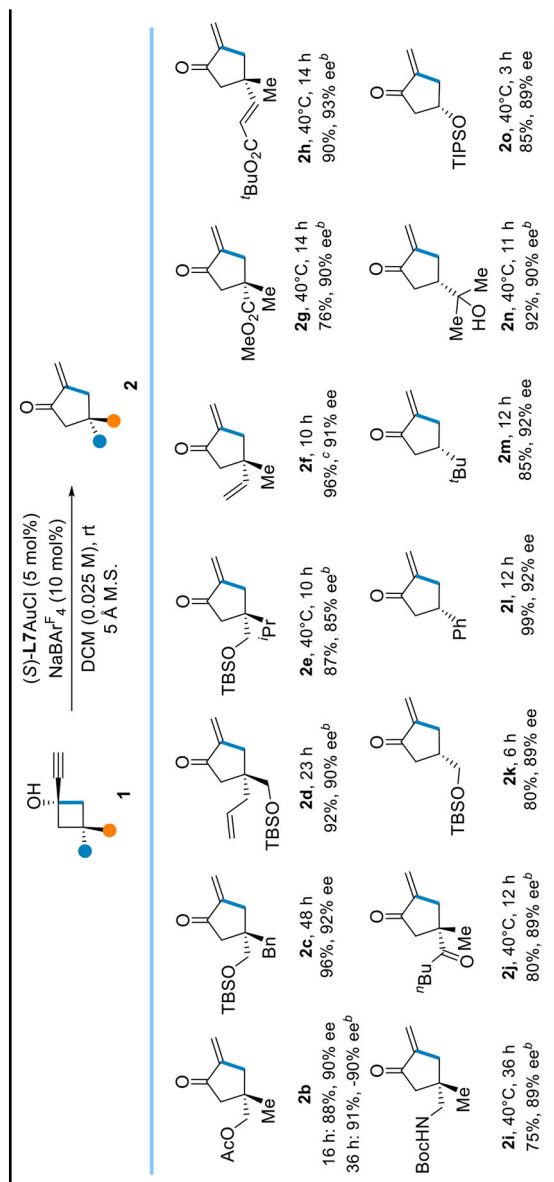
Author Manuscript

Author Manuscript

Author Manuscript

Author Manuscript

Table 2.

Reaction Scope of Desymmetrization<sup>a</sup><sup>a</sup>Reaction run on a 0.20 mmol scale in DCM (0.025 M), isolated yield reported, and the ee values determined by chiral HPLC analysis.<sup>b</sup>Reaction was run at 40 °C.<sup>c</sup><sup>1</sup>H NMR yield.